

# Holographic $f(T)$ -gravity model with power-law entropy correction

K. Karami<sup>1\*</sup>, S. Asadzadeh<sup>1</sup>, A. Abdolmaleki<sup>1</sup>, Z. Safari<sup>2</sup>

<sup>1</sup>Department of Physics, University of Kurdistan, Pasdaran St., Sanandaj, Iran

<sup>2</sup>Research Institute for Astronomy and Astrophysics of Maragha (RIAAM), Maragha, Iran

August 31, 2018

## Abstract

Using a correspondence between the  $f(T)$ -gravity with the power-law entropy corrected version of the holographic dark energy model, we reconstruct the holographic  $f(T)$ -gravity model with power-law entropy correction. We fit the model parameters by using the latest observational data including type Ia supernovae, baryon acoustic oscillation, cosmic microwave background, and Hubble parameter data. We also check the viability of our model using a cosmographic analysis approach. Using the best-fit values of the model, we obtain the evolutionary behaviors of the effective torsion equation of state parameter of the power-law entropy corrected holographic  $f(T)$ -gravity model as well as the deceleration parameter of the universe. We also investigate different energy conditions in our model. Furthermore, we examine the validity of the generalized second law of gravitational thermodynamics. Finally, we point out the growth rate of matter density perturbation in our model. We conclude that in power-law entropy corrected holographic  $f(T)$ -gravity model, the universe begins a matter dominated phase and approaches a de Sitter regime at late times, as expected. It also can justify the transition from the quintessence state to the phantom regime in the near past as indicated by recent observations. Moreover, this model is consistent with current data, passes the cosmographic test and fits the data of the growth factor well as the  $\Lambda$ CDM model.

**PACS numbers:** 04.50.Kd, 95.36.+x

**Keywords:** Modified theories of gravity, Dark energy

---

\*KKarami@uok.ac.ir

# 1 Introduction

Astronomical data from the type Ia supernovae (SNeIa), cosmic microwave background (CMB) and baryon acoustic oscillation (BAO), etc., have implied that the current expansion of the universe is accelerating [1]. The proposals that have been put forth to explain this observed phenomenon can basically be classified into two categories. One is to introduce some unknown matters with negative pressure called “dark energy” (DE) in the framework of Einstein’s general relativity (for reviews on DE, see e.g. [2]). Another alternative to account for the current accelerating cosmic expansion is to modify the gravitational theory called “dark gravity” (see e.g. [3] for a review on modified gravity).

Among the many dynamical DE models, a class with feature of quantum gravity looks very special and attractive. Such class of models, usually called holographic DE (HDE) [4], has been motivated from the holographic principle [5]. The energy density of the HDE is given by

$$\rho_\Lambda = 3c^2 M_P^2 L^{-2}, \quad (1)$$

where  $c$  is a numerical constant [4]. The HDE models have been studied widely in the literature [6, 7, 8, 9, 10, 11, 12, 13, 14]. The derivation of the HDE density depends on the entropy-area relationship  $S_{\text{BH}} = A/(4G)$ , with  $A \sim L^2$  which is the area of horizon. This definition for the entropy in the presence of quantum effects can be modified. The quantum correction to the horizon entropy reads [15]

$$S_A = \frac{A}{4G} \left[ 1 - K_\alpha A^{1-\frac{\alpha}{2}} \right], \quad (2)$$

where  $\alpha$  is a dimensionless parameter and

$$K_\alpha = \frac{\alpha(4\pi)^{\frac{\alpha}{2}-1}}{(4-\alpha)r_c^{2-\alpha}}, \quad (3)$$

here  $r_c$  is the crossover scale. The second term in Eq. (2) can be regarded as a power-law correction to the Bekenstein-Hawking entropy-area relation  $S_A = S_{\text{BH}} = A/(4G)$ , resulting from entanglement, when the wave-function of the field is chosen to be a superposition of ground state and excited state [15, 16, 17].

Following the derivation of the HDE [6] and taking the relation (2) into account, the HDE density will be modified. The result yields the power-law entropy-corrected HDE (PLECHDE) density as [18]

$$\rho_\Lambda = 3c^2 M_P^2 L^{-2} - \beta M_P^2 L^{-\alpha}, \quad (4)$$

where  $\beta$  is a dimensional constant. Karami et al. [19] investigated the validity of the generalized second law of gravitational thermodynamics on the apparent horizon for the power-law corrected entropy-area relation (2) and concluded that the GSL is satisfied from the past to the present for  $\alpha < 2$  and it is violated in the future. In section 4, we will use the current observational data to constrain the parameter  $\alpha$ . Karami et al. [19], interestingly enough, also found that for the PLECHDE model (4) which is the power-law entropy-corrected version of the HDE model (1), the identification of IR cut-off with Hubble horizon,  $L = H^{-1}$ , can lead to a phantom accelerating universe. This is in contrast to the ordinary HDE where its equation of state parameter behaves like the dust (or dark) matter if one chooses  $L = H^{-1}$ .

In the framework of modified gravity, recently a new dark gravity theory, namely the so-called  $f(T)$  theory, attracted much attention in the community, where  $T$  is the torsion scalar [20, 21]. It has been demonstrated that the  $f(T)$  theory can not only explain the present cosmic acceleration with no need of DE [21], but also provide an alternative to inflation without an

inflaton [20].  $f(T)$  theory is based on the old idea of teleparallel gravity (TG) [22], in which the Weitzenböck connection rather than the Levi-Civita connection is used. As a result, the space-time has only torsion and thus is curvature-free. Although TG is closely related to standard GR, differing only in terms involving total derivatives in the action, i.e. boundary terms [23], there are some fundamental conceptual differences between them. According to GR, gravity curves the space-time and shapes the geometry. In TG however torsion does not shape the geometry but instead acts as a force. It means that in TG there are no geodesic equations but there are force equations much like the Lorentz force in electrodynamics [24]. In the literature, several gravitational theories with torsion were proposed (see e.g. [25] for a good review on extended theories of gravity).

$f(T)$  theory is obtained by extending the action of TG in analogy to the  $f(R)$  theory. An important advantage of  $f(T)$  theory is that its field equations are second order as opposed to the fourth order equations of  $f(R)$  gravity [26]. This feature has led to a rapidly increasing interest in the literature. Numerous features of theoretical and observational interests have been studied in this gravity model already including some viable phenomenological  $f(T)$  models [27], observational constraints [28], cosmological perturbations and growth factor of matter perturbations [29], matter stability [30], Birkhoff's theorem [31], Static solutions with spherical symmetry [32], cosmography [33, 34], and thermodynamical description of  $f(T)$ -gravity [35, 36]. For reviews on other aspects of TG and  $f(T)$ -gravity, see [37, 38, 39].

In the present work, our aim is to reconstruct a  $f(T)$ -gravity model without resorting to any additional DE, that is, considering that the PLECHDE is effectively described by the modification of the gravity with respect to the TG. To do so, in section 2, we briefly review the  $f(T)$ -gravity in a spatially flat FRW universe filled only with the pressureless matter. In section 3, we reconstruct a  $f(T)$  model according to the evolution of PLECHDE density. In section 4, we fit this model and give the constraints on model parameters, with current observational data including SNeIa, CMB, BAO and observational Hubble data (OHD). In section 5, we give the numerical results. In section 6, we check the viability of our model using the cosmographic analysis method. In section 7, the validity of the generalized second law of gravitational thermodynamics for our  $f(T)$  model is examined. In section 8, we study the growth of structure formation in our model. Section 9 is devoted to conclusions.

## 2 The $f(T)$ theory of gravity

The modified teleparallel action of a generic  $f(T)$  model with the matter Lagrangian  $L_m$  is [20, 21]

$$I = \frac{1}{2k^2} \int d^4x e [f(T) + L_m], \quad (5)$$

where  $k^2 = M_P^{-2} = 8\pi G$ ,  $e = \det(e_\mu^i) = \sqrt{-g}$  and  $T$  is the torsion scalar. Here  $e_\mu^i$  is the vierbein field which uses as dynamical object in TG.

The modified Friedmann equations in the case of  $f(T)$ -gravity for the spatially flat FRW universe are given by [26, 36]

$$\frac{3}{k^2} H^2 = \rho_m + \rho_T, \quad (6)$$

$$\frac{1}{k^2} (2\dot{H} + 3H^2) = -(p_m + p_T), \quad (7)$$

where

$$\rho_T = \frac{1}{2k^2} (2T f_T - f - T), \quad (8)$$

$$p_T = -\frac{1}{2k^2}[-8\dot{H}T f_{TT} + (2T - 4\dot{H})f_T - f + 4\dot{H} - T], \quad (9)$$

$$T = -6H^2, \quad (10)$$

and  $H = \dot{a}/a$  denotes the Hubble parameter. Here  $\rho_m$  and  $p_m$  are the energy density and pressure of the matter inside the universe, respectively. Also  $\rho_T$  and  $p_T$  are the torsion contributions to the energy density and pressure. The energy conservation laws are given by

$$\dot{\rho}_m + 3H(\rho_m + p_m) = 0, \quad (11)$$

$$\dot{\rho}_T + 3H(\rho_T + p_T) = 0. \quad (12)$$

By using Eqs. (8) and (9), one can define the effective torsion equation of state (EoS) parameter as [26, 36]

$$\omega_T = \frac{p_T}{\rho_T} = -1 + \frac{8\dot{H}T f_{TT} + 4\dot{H}f_T - 4\dot{H}}{2T f_T - f - T}. \quad (13)$$

With the help of Eqs. (6), (8) and (10) one can get

$$\rho_m = \frac{1}{16\pi G}(f - 2T f_T). \quad (14)$$

For the pressureless matter, i.e.  $p_m = 0$ , from Eqs. (6) to (9) one can obtain

$$\dot{H} = -\frac{4\pi G \rho_m}{f_T + 2T f_{TT}}. \quad (15)$$

Inserting Eq. (14) into (15) and using  $\dot{T} = -12H\dot{H}$  gives

$$\dot{T} = 3H \left( \frac{f - 2T f_T}{f_T + 2T f_{TT}} \right). \quad (16)$$

Using the above relation, the effective EoS parameter (13) yields

$$\omega_T = -\frac{f/T - f_T + 2T f_{TT}}{(f_T + 2T f_{TT})(f/T - 2f_T + 1)}. \quad (17)$$

It is also interesting to study the behavior of the deceleration parameter defined as

$$q = -1 - \frac{\dot{H}}{H^2}, \quad (18)$$

which can be compared with the observations. Using Eqs. (10) and (16) the deceleration parameter (18) leads to

$$q = 2 \left( \frac{f_T - T f_{TT} - \frac{3f}{4T}}{f_T + 2T f_{TT}} \right). \quad (19)$$

### 3 Power-law entropy corrected holographic $f(T)$ -gravity model

The dark torsion contribution in  $f(T)$ -gravity can justify the observed acceleration of the universe without resorting to the DE. This motivates us to reconstruct a  $f(T)$ -gravity model according to the PLECHDE model. Following [19, 18], the PLECHDE density with the Hubble IR cut-off  $L = H^{-1}$  is given by

$$\rho_\Lambda = \frac{3c^2}{k^2} H^2 - \frac{\beta}{k^2} H^\alpha, \quad (20)$$

where  $c$ ,  $\alpha$  and  $\beta$  are constants. For  $\beta = 0$  the above equation transforms to the well-known HDE density with the Hubble horizon [4].

Replacing  $H = (-\frac{T}{6})^{1/2}$  into (20) yields

$$\rho_\Lambda = -\frac{c^2}{2k^2}T - \frac{\gamma}{2k^2}(-T)^{\frac{\alpha}{2}}, \quad (21)$$

where

$$\gamma = \frac{2\beta}{6^{\alpha/2}}. \quad (22)$$

Equating (8) with (21), i.e.  $\rho_T = \rho_\Lambda$ , gives the following differential equation

$$2Tf_T - f - (1 - c^2)T + \gamma(-T)^{\frac{\alpha}{2}} = 0. \quad (23)$$

Solving Eq. (23) yields the power-law entropy corrected holographic (PLECH)  $f(T)$ -gravity model as

$$f(T) = \epsilon\sqrt{-T} + (1 - c^2)T + \frac{\gamma}{1 - \alpha}(-T)^{\frac{\alpha}{2}}, \quad (24)$$

where  $\epsilon$  is an integration constant that can be determined from a boundary condition. Following [33] to recover the present day value of Newtonian gravitational constant we need to have

$$f_T(T_0) = 1, \quad (25)$$

where  $T_0 = -6H_0^2$  is the torsion scalar at the present time. Applying the above boundary condition to the solution (24) one can obtain

$$\epsilon = -2\sqrt{6}H_0 \left[ c^2 + \frac{\gamma\alpha}{2(1 - \alpha)}(6H_0^2)^{\frac{\alpha}{2}-1} \right]. \quad (26)$$

Note that the parameter  $\gamma$  can be obtained by inserting Eq. (24) into the modified Friedmann equation (6). Solving the resulting equation for the present time gives

$$\gamma = \frac{\Omega_{m_0} + c^2 - 1}{(6H_0^2)^{\frac{\alpha}{2}-1}}, \quad (27)$$

Replacing Eq. (27) into (26) yields

$$\epsilon = \sqrt{6}H_0 \left[ \frac{\alpha(\Omega_{m_0} - 1) + c^2(2 - \alpha)}{\alpha - 1} \right]. \quad (28)$$

Using Eqs. (6), (8), (24) and (27) one can obtain the dimensionless Hubble parameter  $E(z; \mathbf{p}) = H(z; \mathbf{p})/H_0$  as

$$E^2(z; \mathbf{p}) = \Omega_{m_0}(1 + z)^3 + c^2E^2(z; \mathbf{p}) + (1 - \Omega_{m_0} - c^2)E^\alpha(z; \mathbf{p}). \quad (29)$$

where  $\Omega_{m_0}h^2 = 0.1352 \pm 0.0036$  (68% CL) is the present value of the dimensionless matter energy density and  $H_0 = 70.2 \pm 1.4 \text{ km s}^{-1} \text{ Mpc}^{-1}$  (68% CL) is the present Hubble constant which has been updated in the 7-year WMAP (WMAP7) data [40]. Also  $\mathbf{p}$  indicate model parameters. Thus, throughout this work we fix the dimensionless matter energy density and Hubble parameters at  $\Omega_{m_0}h^2 = 0.1352$  and  $H_0 = 70.2$ . With  $\Omega_{m_0}$  and  $H_0$  being determined by independent measurements, in the next section we will use the cosmic observations to constrain the PLECH  $f(T)$ -gravity model parameters  $\mathbf{p} = (\alpha, c^2)$ .

Inserting Eq. (24) into (17) gives the EoS parameter of the torsion contribution as

$$\omega_T = \frac{\gamma(\alpha - 2)(-T)^{\frac{\alpha}{2}+1}}{\left[ c^2 T + \gamma(-T)^{\frac{\alpha}{2}} \right] \left[ 2(c^2 - 1)T + \alpha\gamma(-T)^{\frac{\alpha}{2}} \right]}. \quad (30)$$

Inserting Eq. (24) into (19), the deceleration parameter takes the form

$$q = \frac{(c^2 - 1)T - \gamma(\alpha - 3)(-T)^{\frac{\alpha}{2}}}{2(c^2 - 1)T + \alpha\gamma(-T)^{\frac{\alpha}{2}}}. \quad (31)$$

## 4 Observational constraints

Here, we fit the free parameters of the PLECH  $f(T)$ -gravity model by using the recent observational data including SNeIa, BAO, CMB and OHD.

### 4.1 Type Ia Supernovae (SNeIa)

SNeIa can be used to directly measure the expansion rate of the universe up to high redshift. We use the Union2.1 compilation [41] containing 580 SNeIa. It is an updated version of the Union2 compilation [42]. Constraints from the SNeIa data can be obtained by fitting the distance modulus  $\mu(z)$ . A distance modulus can be calculated as [43, 44]

$$\mu_{\text{th}}(z) = 5 \log_{10} D_L(z) + \mu_0, \quad (32)$$

where  $\mu_0 = 42.38 - 5 \log_{10} h$  and  $h$  is the Hubble constant  $H_0$  in units of  $100 \text{ km s}^{-1} \text{ Mpc}^{-1}$ . Also the Hubble-free luminosity distance  $D_L(z)$  for the flat universe is given by

$$D_L(z) = (1 + z) \int_0^z \frac{dz'}{E(z'; \mathbf{p})}. \quad (33)$$

Using SNeIa data, theoretical model parameters can be determined by minimizing [43, 44]

$$\tilde{\chi}_{\text{SN}}^2 = A - \frac{B^2}{C}, \quad (34)$$

where

$$A = \sum_{i=1}^{580} [\mu_{\text{obs}}(z_i) - \mu_{\text{th}}(z_i)]^2 / \sigma_i^2, \quad (35)$$

$$B = \sum_{i=1}^{580} [\mu_{\text{obs}}(z_i) - \mu_{\text{th}}(z_i)] / \sigma_i^2, \quad (36)$$

$$C = \sum_{i=1}^{580} 1 / \sigma_i^2, \quad (37)$$

and  $\sigma_i$  stands for the  $1\sigma$  uncertainty associated to the  $i$ th data point.

## 4.2 Baryon Acoustic Oscillations (BAO)

BAO can be traced to pressure waves at the recombination epoch generated by cosmological perturbations in the primeval baryon-photon plasma. They have been revealed by a distinct peak in the large scale correlation function measured from the luminous red galaxies sample of the Sloan Digital Sky Survey (SDSS) at  $z_b = 0.35$  [45, 46]. Using the BAO data, one can minimize the  $\chi_{\text{BAO}}^2$  defined as [45, 46],

$$\chi_{\text{BAO}}^2 = \frac{[A_{\text{obs}} - A_{\text{th}}]^2}{\sigma_A^2}, \quad (38)$$

where

$$A_{\text{th}} = \sqrt{\Omega_{m_0}} E(z_b; \mathbf{p})^{-1/3} \left[ \frac{1}{z_b} \int_0^{z_b} \frac{dz'}{E(z'; \mathbf{p})} \right]^{2/3}, \quad (39)$$

is the theoretical distance parameter. Here  $A_{\text{obs}} = 0.469(n_s/0.98)^{-0.35} \pm 0.017$  is measured from the SDSS data [46] and the scalar spectral index  $n_s$  is taken to be 0.968, which has been updated from the WMAP7 data [40].

## 4.3 CMB shift parameter

The structure of the anisotropies of the CMB radiation depends on two eras in cosmology, i.e., the last scattering era and today. They can also be applied to limit the cosmological models by minimizing

$$\chi_{\text{CMB}}^2 = \frac{[R_{\text{obs}} - R_{\text{th}}]^2}{\sigma_R^2}. \quad (40)$$

Here the shift parameter  $R$  of the CMB is related to the position of the first acoustic peak in the power spectrum of the temperature anisotropies and given by [47, 48]

$$R_{\text{th}} = \sqrt{\Omega_{m_0}} \int_0^{z_{\text{rec}}} \frac{dz'}{E(z'; \mathbf{p})}, \quad (41)$$

where  $z_{\text{rec}} \simeq 1091.3$  is the redshift at the recombination epoch [40]. Also the observational value of  $R_{\text{obs}}$  has been updated to  $1.725 \pm 0.018$  from the WMAP7 data [40].

## 4.4 Observational Hubble Data (OHD)

We use the compilation of Hubble parameter measurements estimated with the differential evolution of passively evolving early-type galaxies as cosmic chronometers. For the Hubble parameter

$$H(z) = -\frac{1}{1+z} \frac{dz}{dt}, \quad (42)$$

if  $dz/dt$  is known,  $H(z)$  is obtained directly [49]. Observed values of  $H(z)$  can be used to estimate the free parameters of the model by minimizing the quantity [50]

$$\chi_{\text{OHD}}^2 = \sum_{i=1}^{15} \frac{[H_{\text{obs}}(z_i) - H_{\text{th}}(z_i, \mathbf{p})]^2}{\sigma_i^2}, \quad (43)$$

where  $\sigma_i^2$  are the measurement variances. The 12 observational data of Hubble parameter [51]-[53] are listed in Table 1. We also use three more additional data:  $H(z = 0.24) = 79.69 \pm 2.32$ ,  $H(z = 0.34) = 83.8 \pm 2.96$ , and  $H(z = 0.43) = 86.45 \pm 3.27$  given by [54].

As the relative likelihood function is defined by  $\mathcal{L} = e^{-(\chi_{\text{total}}^2 - \chi_{\text{min}}^2)/2}$  [55], the best-fit value of the model parameters follows from minimizing the sum

$$\chi_{\text{total}}^2 = \tilde{\chi}_{\text{SN}}^2 + \chi_{\text{BAO}}^2 + \chi_{\text{CMB}}^2 + \chi_{\text{OHD}}^2. \quad (44)$$

## 5 Numerical results

Now, we discuss the constraints on model parameters of PLECH  $f(T)$ -gravity model (24) by using the recent observational data including SNeIa, CMB, BAO and OHD.

The results are summarized in Table 2, where we also list the best-fit value of the corresponding parameter of the  $\Lambda$ CDM model for comparison. At 68.3% and 95.4% confidence levels (CLs), we obtain the best-fit value  $\alpha = -0.18_{-0.34}^{+0.27}(1\sigma)_{-0.77}^{+0.48}(2\sigma)$  and  $c^2 = 0.025_{-0.025}^{+0.035}(1\sigma)_{-0.025}^{+0.067}(2\sigma)$  for the full data sets including SNeIa+CMB+BAO+OHD. The total  $\chi^2$  of the best-fit value of the PLECH  $f(T)$ -gravity model is  $\chi_{\text{min}}^2 = 571.026$  for the full data sets with degrees of freedom (dof) = 597. The reduced  $\chi^2$  is 0.956, which is acceptable, but  $\chi_{\text{min}}^2$  is smaller than the one for the  $\Lambda$ CDM model,  $\chi_{\Lambda\text{CDM}}^2 = 571.306$  and  $\Omega_{m_0} = 0.272_{-0.012}^{+0.014}(1\sigma)_{-0.025}^{+0.027}(2\sigma)$ , for the same data sets. The marginalized relative likelihood functions  $\mathcal{L}(\alpha)$  and  $\mathcal{L}(c^2)$  are shown in Figs. 1 and 2, respectively. Figure 3 shows the constraint on the PLECHDE parameter space  $\alpha - c^2$  at  $1\sigma$  and  $2\sigma$  CLs, using the full data sets.

The evolution of the PLECH  $f(T)$ -gravity model, Eq. (24), versus  $z$  is shown in Fig. 4, where we also plot  $f(T) = T$  corresponding to the case of TG for comparison. Figure 4 shows that the PLECH  $f(T)$ -gravity model (24) satisfies the condition

$$\lim_{|T| \rightarrow \infty} f/T \rightarrow 1,$$

at high redshift which is compatible with the primordial nucleosynthesis and CMB constraints [26].

The time evolution of the EoS parameter (30) for the best-fit values of model parameters is plotted in Fig. 5. It shows that at early time ( $z \gg 1$ ) we have  $\omega_T \rightarrow -0.3$  and at late time ( $z = -1$ ) we get  $\omega_T \rightarrow -1$  which acts like the  $\Lambda$ CDM model. Also at present time we have  $\omega_{T_0} = -1.01$  which is in good agreement with the recent observational result  $\omega_{T_0} = -0.93 \pm 0.13$  (68% CL) deduced from the WMAP7 data [40]. Figure 5 clears that the EoS parameter of the PLECH  $f(T)$ -gravity model crosses the phantom divide line from the values greater than  $-1$  (quintessence phase) to smaller than  $-1$  (phantom phase) at  $z = 0.81$  which is compatible with observations [56].

In Fig. 6, we plot the evolutionary behavior of the deceleration parameter of the universe, Eq. (31), with the best-fit values of the PLECH  $f(T)$ -gravity and  $\Lambda$ CDM models. Figure 6 shows that very similar to the  $\Lambda$ CDM model the universe transits from an early matter dominant regime to the de Sitter phase in the future, as expected. The accelerating expansion begins at transition redshift  $z_t = 0.73$ , which is later than what the  $\Lambda$ CDM model predicts,  $z_t^{\Lambda\text{CDM}} = 0.75$ . The current best fit value of the deceleration parameter in the PLECH  $f(T)$ -gravity model is obtained as  $q_0 = -0.6$  which indicates the expansion rhythm of the current universe. This is in agreement with the recent observational constraint  $q_0 = -0.43_{-0.17}^{+0.13}$  (68% CL) obtained by the cosmography [33].

The evolutions of  $\rho_T + p_T$ ,  $\rho_T + 3p_T$  and  $(\rho_T, |p_T|)$  versus  $z$  are plotted in Figs. 7, 8 and 9, respectively. Figures show that: (i) the null energy condition (NEC), i.e.  $\rho_T + p_T \geq 0$ , is violated when  $z < 0.81$  (see Fig. 7). (ii) The strong energy condition (SEC), i.e.  $\rho_T + p_T \geq 0$  and  $\rho_T + 3p_T \geq 0$ , is violated when  $z < 4.47$  (see Fig. 8). (iii) The weak energy condition

(WEC), i.e.  $\rho_T + p_T \geq 0$  and  $\rho_T \geq 0$ , is violated when  $z < 0.81$  (see Fig. 9). (iv) The dominant energy condition (DEC), i.e.  $\rho_T \geq 0$  and  $\rho_T \geq |p_T|$ , is violated when  $z < 0.81$  (see Fig. 9).

## 6 Cosmographic analysis

Here we use the cosmographic constraints to check the viability of  $f(T)$  model without the need of explicitly solving the field equations and fitting the data [33]. From Eqs. (27) and (28),  $\gamma$  and  $\epsilon$  are known. This yields the  $f_i = f^{(i)}(T_0)/(6H_0^2)^{-(i-1)}$  values, given by Eqs. (4.23)-(4.26) in [33], for  $i = (2, 3, 4, 5)$  where  $f^{(i)}(T) = d^i f/dT^i$  to be expressed as function of  $\alpha$  and  $c^2$  when we fix  $\Omega_{m_0} = 0.1352/h^2$  from the WMAP7 data. Following [33] for each  $f_2$  and  $f_3$  values of the sample obtained above from the cosmographic parameters analysis, we solve  $\hat{f}_2(\alpha, c^2) = f_2$  and  $\hat{f}_3(\alpha, c^2) = f_3$  to derive  $\alpha$  and  $c^2$  and estimate the theoretically expected values for the other derivatives ( $f_4, f_5$ ). The median is obtained as

$$\begin{aligned} f_4 &= 1.581 \\ f_5 &= 5.456. \end{aligned} \quad (45)$$

The above values for  $(f_4, f_5)$  take place in the 68% CL in Table II in [33]. Hence, we conclude that the PLECH  $f(T)$ -gravity model passes the cosmographic test.

## 7 Generalized second law of thermodynamics (GSL)

Here, we investigate the validity of the GSL of gravitational thermodynamics for PLECH  $f(T)$ -gravity model. Within the framework of  $f(T)$ -gravity, the GSL is given by [36]

$$T_A \dot{S}_{\text{tot}} = \frac{9}{8G} \left( \frac{f - 2T f_T}{f_T + 2T f_{TT}} \right) \left[ 4f_{TT} + \left( \frac{f - 2T f_T}{f_T + 2T f_{TT}} \right) \left( \frac{f_T + 5T f_{TT}}{T^2} \right) \right], \quad (46)$$

where  $S_{\text{tot}} = S_m + S_A$  is the total entropy due to contributions of both the matter and horizon. Also  $T_A$  is the Hawking temperature [57]. In  $f(T)$ -gravity, the horizon entropy

$$S_A = \frac{A f_T}{4G}, \quad (47)$$

where  $A = 4\pi \tilde{r}_A^2$ , is valid only when  $f_{TT}$  is small [35]. We plot  $f_{TT}$  versus  $z$  for our model (24) in Fig. 10 which shows that the  $f_{TT}$  is very small. Hence Eq. (47) is valid for PLECH  $f(T)$ -gravity model.

The GSL, Eq. (46), for the PLECH  $f(T)$ -gravity model (24) reads

$$GT_A \dot{S}_{\text{tot}} = \frac{\text{I}}{8(\alpha - 1) [2(c^2 - 1)T + \alpha\gamma(-T)^{\alpha/2}]^2 T}, \quad (48)$$

where

$$\begin{aligned} \text{I} = & - 9 \left[ (c^2 - 1)T + \gamma(-T)^{\alpha/2} \right] \left\{ 4(\alpha - 1)(c^2 - 1)^2 T^2 \right. \\ & + (c^2 - 1) \left[ (-4 + \alpha(4 + \alpha))\gamma(-T)^{\alpha/2} - (\alpha - 1)\epsilon\sqrt{-T} \right] T \\ & \left. + \gamma \left[ -\alpha\gamma(8 + \alpha(-9 + 2\alpha))(-T)^{\alpha/2} + \epsilon(-3 + 5\alpha - 2\alpha^2)\sqrt{-T} \right] (-T)^{\alpha/2} \right\}. \end{aligned} \quad (49)$$

The variation of the GSL (48) versus  $z$  is plotted in Fig. 11. Figure shows that the GSL for our model is satisfied from the early times to the present epoch. But in the future the GSL is violated for  $z < -0.32$ . These are in good agreement with those obtained by [19] for the power-law corrected entropy-area relation (2).

## 8 The growth of structure formation

Here, we investigate the growth rate of matter density perturbation in PLECH  $f(T)$ -gravity model. In  $f(T)$ -gravity, the matter density contrast  $\delta_m = \delta\rho_m/\rho_m$  satisfies [58]

$$\ddot{\delta}_m + 2H\dot{\delta}_m - 4\pi G_{\text{eff}}\rho_m\delta_m = 0, \quad (50)$$

where  $G_{\text{eff}} = \frac{G}{f_T}$  is the effective Newton's constant. Now we define a new variable  $g(a)$ , namely  $g(a) \equiv \delta_m/a$  which does not depend on  $a$  during the matter era. Thus the initial conditions are  $g(a_i) = 1$  and  $\frac{dg}{d\ln a}|_{a=a_i} = 0$ , where  $a_i = 1/31$  (i.e.,  $z = 30$ ) [58]. Equation (50) in terms of  $g(a)$  becomes

$$\frac{d^2g}{d\ln a^2} + \left(4 + \frac{\dot{H}}{H^2}\right) \frac{dg}{d\ln a} + \left(3 + \frac{\dot{H}}{H^2} - \frac{4\pi G_{\text{eff}}\rho_m}{H^2}\right) g = 0. \quad (51)$$

From Eqs. (18), (19), (24), (27) and (28) one can get

$$\frac{\dot{H}}{H^2} = -\frac{3}{2} \left( \frac{2f_T - f/T}{f_T + 2Tf_{TT}} \right) = -\frac{3}{2} \left[ \frac{1 - c^2 + (\Omega_{m_0} + c^2 - 1)E^{\alpha-2}}{1 - c^2 + \frac{\alpha}{2}(\Omega_{m_0} + c^2 - 1)E^{\alpha-2}} \right], \quad (52)$$

where  $E(z) = H(z)/H_0$  is given by Eq. (29). Also with the help of Eq. (15) and (52) one can obtain

$$\frac{4\pi G_{\text{eff}}\rho_m}{H^2} = \frac{3}{2} \left( 2 - \frac{f}{Tf_T} \right) = \frac{3}{2} \left[ \frac{(1 - c^2)E + (\Omega_{m_0} + c^2 - 1)E^{\alpha-1}}{c^2 + (1 - c^2)E + \frac{1}{2} \left( \frac{\alpha}{\alpha-1} \right) (\Omega_{m_0} + c^2 - 1)(E^{\alpha-1} - 1)} \right]. \quad (53)$$

Taking the derivative of Eq. (29) with respect to  $\ln a$  gives

$$\frac{d\ln E}{d\ln a} = -\frac{3}{2} \left[ \frac{1 - c^2 + (\Omega_{m_0} + c^2 - 1)E^{\alpha-2}}{1 - c^2 + \frac{\alpha}{2}(\Omega_{m_0} + c^2 - 1)E^{\alpha-2}} \right], \quad (54)$$

with the initial condition  $E(a = 1) = 1$ . Note that to obtain the evolutionary behavior of  $g(a)$ , we need to solve Eqs. (51) and (54), numerically.

In Fig. 12, we plot the evolutionary behavior of the  $g(a) = \delta_m/a$  with the best-fitting values of the PLECH  $f(T)$ -gravity model,  $\Lambda$ CDM model, and DE model with the same EoS in GR. Note that the variation of  $g(a)$  for the DE scenario in GR with the same EoS as the effective DE in  $f(T)$  is obtained by replacing  $G_{\text{eff}}$  with  $G$  in Eq. (51). Figure 12 shows that: (i)  $g(a)$  for the three models starts from an early matter dominant phase, i.e.  $g \simeq 1$ , and decreases during history of the universe. (ii) For a given  $z$ ,  $g(a)$  in the PLECH  $f(T)$ -gravity model like the  $\Lambda$ CDM model gets greater than that in the DE model with the same EoS in GR.

Figure 13 shows the evolutionary behavior of the growth factor  $f(z)$  defined as [59]

$$f(z) = \frac{d\ln \delta_m}{d\ln a} = -(1+z) \frac{d\ln \delta_m}{dz}, \quad (55)$$

with the best-fitting values of the PLECH  $f(T)$ -gravity model,  $\Lambda$ CDM model, and DE model with the same EoS in GR. The growth factor data are listed in Table 3. Figure 13 shows that the PLECH  $f(T)$ -gravity model fits the data of the growth factor well as the  $\Lambda$ CDM model.

## 9 Conclusions

Within the framework of  $f(T)$  modified teleparallel theory, we reconstructed a  $f(T)$  model according to the PLECHDE model. We fitted the model with current observational data, including SNeIa, BAO, CMB and OHD. We obtained the constraint results of PLECH  $f(T)$ -gravity model parameters,  $\alpha = -0.18_{-0.34}^{+0.27}(1\sigma)_{-0.77}^{+0.48}(2\sigma)$  and  $c^2 = 0.025_{-0.025}^{+0.035}(1\sigma)_{-0.025}^{+0.067}(2\sigma)$  for the full data sets. The minimal  $\chi^2$  gives  $\chi_{\min}^2 = 571.026$  with dof= 597. The reduced  $\chi^2$  equals to 0.956 which is acceptable. The  $\chi_{\min}^2$  is slightly smaller than the one for the  $\Lambda$ CDM model,  $\chi_{\Lambda\text{CDM}}^2 = 571.306$ , for the same data sets. Using the best-fit values of the PLECH  $f(T)$ -gravity model parameters, we also studied the evolutionary behaviors of the effective torsion EoS parameter of PLECH  $f(T)$ -gravity model, the deceleration parameter of the universe and different energy conditions.

Using a cosmographic analysis approach, we also checked the viability of our model without the need of explicitly solving the field equations and fitting the data. We further examined the validity of the GSL of gravitational thermodynamics for the PLECH  $f(T)$ -gravity model. Finally, we pointed out the growth of structure formation in our model. Our results show the following.

(i) The condition  $f/T \rightarrow 1$  is satisfied for our model at high redshift ( $|T| \rightarrow \infty$ ) which is compatible with the primordial nucleosynthesis and CMB constraints.

(ii) The effective torsion EoS parameter  $\omega_T$  varies from  $\omega_T > -1$  to  $\omega_T = -1$ . At late time, it behaves like the  $\Lambda$ CDM model. For the present time, we obtain  $\omega_{T_0} = -1.01$  which acts like phantom universe and it is in good agreement with the recent observational result deduced from the WMAP7 data [40]. Also  $\omega_T$  shows a transition from the quintessence phase ( $\omega_T > -1$ ) to the phantom regime ( $\omega_T < -1$ ) at  $z = 0.81$  which is compatible with observations [56].

(iii) The variation of the deceleration parameter  $q$  shows that the universe transits from an early matter dominant epoch ( $q = 0.5$ ) to the de Sitter era ( $q = -1$ ) in the future, as expected. The accelerating expansion begins at transition redshift  $z_t = 0.73$ , which is later than what the  $\Lambda$ CDM model predicts,  $z_t^{\Lambda\text{CDM}} = 0.75$ . The deceleration parameter  $q_0 = -0.6$  obtained at the present is compatible with the recent observational constraint obtained by the cosmography [33].

(iv) The NEC, WEC and DEC are violated for  $z < 0.81$  when the universe enters the phantom phase. Also the SEC does not hold for  $z < 4.47$ .

(v) Cosmographic analysis shows that the PLECH  $f(T)$ -gravity model is favored by the observational data.

(vi) The GSL of gravitational thermodynamics holds for our  $f(T)$  model from the early times to the present epoch. But in the future, the GSL is violated for  $z < -0.32$ .

(vii) The evolution of the growth factor in the PLECH  $f(T)$ -gravity model shows that our model like the  $\Lambda$ CDM model fit the data very well.

## Acknowledgements

The authors thank the referee for his/her valuable comments. The works of K. Karami and Z. Safari have been supported financially by Research Institute for Astronomy and Astrophysics of Maragha (RIAAM) under research project No. 1/2782-44.

## References

- [1] A.G. Riess, et al., *Astron. J.* **116**, 1009 (1998);  
 S. Perlmutter, et al., *Astrophys. J.* **517**, 565 (1999);  
 P. de Bernardis, et al., *Nature* **404**, 955 (2000).

- [2] T. Padmanabhan, Phys. Rep. **380**, 235 (2003);  
P.J.E. Peebles, B. Ratra, Rev. Mod. Phys. **75**, 559 (2003);  
E.J. Copeland, M. Sami, S. Tsujikawa, Int. J. Mod. Phys. D **15**, 1753 (2006);  
M. Li, et al., Commun. Theor. Phys. **56**, 525 (2011).
- [3] S. Capozziello, Int. J. Mod. Phys. D **11**, 483 (2002);  
Y. Sobouti, Astron. Astrophys. **464**, 921 (2007);  
S. Capozziello, M. De Laurentis, V. Faraoni, Open Astron. J. **3**, 49 (2010);  
T. P. Sotiriou, V. Faraoni, Rev. Mod. Phys. **82**, 451 (2010);  
S. Nojiri, S.D. Odintsov, Phys. Rep. **505**, 59 (2011).
- [4] M. Li, Phys. Lett. B **603**, 1 (2004).
- [5] G. 't Hooft, gr-qc/9310026;  
L. Susskind, J. Math. Phys. **36**, 6377 (1995).
- [6] B. Guberina, R. Horvat, H. Nikolic, JCAP **01**, 012 (2007).
- [7] J.D. Bekenstein, Phys. Rev. D **7**, 2333 (1973);  
J.D. Bekenstein, Phys. Rev. D **9**, 3292 (1974);  
J.D. Bekenstein, Phys. Rev. D **23**, 287 (1981);  
J.D. Bekenstein, Phys. Rev. D **49**, 1912 (1994);  
S.W. Hawking, Commun. Math. Phys. **43**, 199 (1975);  
S.W. Hawking, Phys. Rev. D **13**, 191 (1976).
- [8] M. Li, X.D. Li, S. Wang, Y. Wang, X. Zhang, JCAP **12**, 014 (2009).
- [9] M. Li, X.D. Li, S. Wang, X. Zhang, JCAP **06**, 036 (2009).
- [10] S.D.H. Hsu, Phys. Lett. B **594**, 13 (2004);  
K. Enqvist, M.S. Sloth, Phys. Rev. Lett. **93**, 221302 (2004);  
Q.G. Huang, Y. Gong, JCAP **08**, 006 (2004);  
Q.G. Huang, M. Li, JCAP **08**, 013 (2004);  
Y. Gong, Phys. Rev. D **70**, 064029 (2004).
- [11] E. Elizalde, et al., Phys. Rev. D **71**, 103504 (2005);  
X. Zhang, F.Q. Wu, Phys. Rev. D **72**, 043524 (2005);  
B. Guberina, R. Horvat, H. Stefancic, JCAP **05**, 001 (2005);  
J.Y. Shen, et al., Phys. Lett. B **609**, 200 (2005);  
B. Wang, E. Abdalla, R.K. Su, Phys. Lett. B **611**, 21 (2005).
- [12] J.P.B. Almeida, J.G. Pereira, Phys. Lett. B **636**, 75 (2006);  
B. Guberina, R. Horvat, H. Nikolic, Phys. Lett. B **636**, 80 (2006);  
H. Li, Z.K. Guo, Y.Z. Zhang, Int. J. Mod. Phys. D **15**, 869 (2006);  
X. Zhang, Phys. Rev. D **74**, 103505 (2006);  
X. Zhang, F.Q. Wu, Phys. Rev. D **76**, 023502 (2007).
- [13] L. Xu, JCAP **09**, 016 (2009);  
M. Jamil, M.U. Farooq, M.A. Rashid, Eur. Phys. J. C **61**, 471 (2009);  
M. Jamil, M.U. Farooq, Int. J. Theor. Phys. **49**, 42 (2010);  
A. Sheykhi, Phys. Lett. B **681**, 205 (2009);  
A. Sheykhi, Phys. Lett. B **682**, 329 (2010);  
A. Sheykhi, Class. Quantum Grav. **27**, 025007 (2010).

- [14] K. Karami, arXiv:1002.0431;  
 K. Karami, JCAP **01**, 015 (2010);  
 K. Karami, J. Fehri, Phys. Lett. B **684**, 61 (2010);  
 K. Karami, J. Fehri, Int. J. Theor. Phys. **49**, 1118 (2010);  
 K. Karami, A. Abdolmaleki, Phys. Scr. **81**, 055901 (2010).
- [15] D. Saurya, S. Shankaranarayanan, S. Sur, Phys. Rev. D **77**, 064013 (2008).
- [16] S. Das, S. Shankaranarayanan, S. Sur, arXiv:1002.1129.
- [17] S. Das, S. Shankaranarayanan, S. Sur, arXiv:0806.0402.
- [18] A. Sheykhi, M. Jamil, Gen. Relativ. Gravit. **43**, 2661 (2011).
- [19] K. Karami, A. Abdolmaleki, N. Sahraei, S. Ghaffari, JHEP **08**, 150 (2011).
- [20] R. Ferraro, F. Fiorini, Phys. Rev. D **75**, 084031 (2007);  
 R. Ferraro, F. Fiorini, Phys. Rev. D **78**, 124019 (2008).
- [21] G.R. Bengochea, R. Ferraro, Phys. Rev. D **79**, 124019 (2009);  
 G.R. Bengochea, Phys. Lett. B **695**, 405 (2011).
- [22] A. Einstein, Sitzungsber. Preuss. Akad. Wiss. Phys. Math. Kl. 217 (1928);  
 A. Einstein, Sitzungsber. Preuss. Akad. Wiss. Phys. Math. Kl. 401 (1930);  
 A. Einstein, Math. Ann. **102**, 685 (1930).
- [23] C. Moller, Mat. Fys. Skr. Danske Vid. Selsk. **1**, 10 (1961);  
 C. Pellegrini, J. Plebanski, Mat. Fys. Skr. Danske Vid. Selsk. **2**, 4 (1963);  
 C. Moller, K. Dan, Mat. Fys. Skr. Danske Vid. Selsk. **89**, 13 (1978).
- [24] K. Hayashi, T. Nakano, Prog. Theor. Phys. **38**, 491 (1967);  
 K. Hayashi, Phys. Lett. B **69**, 441 (1977);  
 K. Hayashi, T. Shirafuji, Phys. Rev. D **19**, 3524 (1979);  
 K. Hayashi, T. Shirafuji, Phys. Rev. D **24**, 3312 (1981).
- [25] S. Capozziello, M. De Laurentis, Phys. Rep. **509**, 167 (2011).
- [26] P. Wu, H. Yu, Phys. Lett. B **692**, 176 (2010);  
 P. Wu, H. Yu, Eur. Phys. J. C **71**, 1552 (2011).
- [27] E.V. Linder, Phys. Rev. D **81**, 127301 (2010);  
 R.J. Yang, Eur. Phys. J. C **71**, 1797 (2011).
- [28] P. Wu, H. Yu, Phys. Lett. B **693**, 415 (2010);  
 H. Wei, X.P. Ma, H.Y. Qi, Phys. Lett. B **703**, 74 (2011);  
 Y. Zhang, et al., JCAP **07**, 015 (2011).
- [29] S.H. Chen, et al., Phys. Rev. D **83**, 023508 (2011);  
 B. Li, T.P. Sotiriou, J.D. Barrow, Phys. Rev. D **83**, 104017 (2011);  
 J.B. Dent, S. Dutta, E.N. Saridakis, JCAP **01**, 009 (2011);  
 R. Zheng, Q.G. Huang, JCAP **03**, 002 (2011);  
 Y.F. Cai, et al., Class. Quantum Grav. **28**, 215011 (2011).
- [30] A. Behboodi, S. Akhshabi, K. Nozari, Phys. Lett. B **718**, 30 (2012).

- [31] X.H. Meng, Y.B. Wang, Phys. Rev. D **84**, 024042 (2011).
- [32] T. Wang, Phys. Rev. D **84**, 024042 (2011).
- [33] S. Capozziello, et al., Phys. Rev. D **84**, 043527 (2011).
- [34] A. Aviles, A. Bravetti, S. Capozziello, O. Luongo, Phys. Rev. D **87**, 064025 (2013).
- [35] K. Bamba, et al., JCAP **01**, 021 (2011);  
R.X. Miao, M. Li, Y.G. Miao, JCAP **11**, 033 (2011).
- [36] K. Karami, A. Abdolmaleki, JCAP **04**, 007 (2012).
- [37] R. Myrzakulov, Eur. Phys. J. C **71**, 1752 (2011);  
P.Y. Tsyba, et al., Int. J. Theor. Phys. **50**, 1876 (2011);  
M.H. Daouda, M.E. Rodrigues, M.J.S. Houndjo, Eur. Phys. J. C **72**, 1893 (2012).
- [38] R.J. Yang, Europhys. Lett. **93**, 60001 (2011).
- [39] H.M. Sadjadi, Phys. Lett. B **718**, 270 (2012);  
H.M. Sadjadi, Phys. Rev. D **87**, 064028 (2013).
- [40] E. Komatsu, et al., Astrophys. J. Suppl. **192**, 18 (2011).
- [41] N. Suzuki, et al., Astrophys. J. **746**, 85 (2012).
- [42] R. Amanullah, et al., Astrophys. J. **716**, 712 (2010).
- [43] E. Di Pietro, J.F. Claeskens, Mon. Not. Roy. Astron. Soc. **341**, 1299 (2003).
- [44] L. Perivolaropoulos, Phys. Rev. D **71**, 063503 (2005);  
R. Gannouji, D. Polarski, JCAP **05**, 018 (2008).
- [45] M. Tegmark, et al., Astrophys. J. **606**, 702 (2004);  
M. Tegmark, et al., Phys. Rev. D **69**, 103501 (2004);  
U. Seljak, et al., Phys. Rev. D **71**, 103515 (2005);  
M. Tegmark, et al., Phys. Rev. D **74**, 123507 (2006).
- [46] D.J. Eisenstein, et al., Astrophys. J. **633**, 560 (2005).
- [47] Y. Wang, P. Mukherjee, Astrophys. J. **650**, 1 (2006).
- [48] J.R. Bond, G. Efstathiou, M. Tegmark, Mon. Not. Roy. Astron. Soc. **291**, L33 (1997).
- [49] R. Jimenez, A. Loeb, Astrophys. J. **573**, 37 (2002).
- [50] L. Samushia, B. Ratra, Astrophys. J. **650**, L5 (2006).
- [51] D. Stern, et al., arXiv:0907.3149.
- [52] J. Simon, et al., Phys Rev D **71**, 123001 (2005).
- [53] A.G. Riess et al., Astrophys. J. **699**, 539 (2009).
- [54] E. Gaztanaga, A. Cabre, L. Hui, Mon. Not. Roy. Astron. Soc. **399**, 1663 (2009).
- [55] S. Nesseris, L. Perivolaropoulos, Phys. Rev. D **72**, 123519 (2005).

- [56] U. Alam, V. Sahni, A.A. Starobinsky, *JCAP* **06**, 008 (2004);  
D. Huterer, A. Cooray, *Phys. Rev. D* **71**, 023506 (2005);  
Y. Wang, M. Tegmark, *Phys. Rev. D* **71**, 103513 (2005).
- [57] R.G. Cai, S.P. Kim, *JHEP* **02**, 050 (2005).
- [58] R. Zheng, Q. Huang, *JCAP* **03**, 002 (2011).
- [59] P.J.E. Peebles, *Principles of Physical Cosmology*, Princeton University Press, Princeton New Jersey (1993).
- [60] L. Verde, et al., *Mon. Not. Roy. Astron. Soc.* **335**, 432 (2002);  
E. Hawkins, et al., *Mon. Not. Roy. Astron. Soc.* **346**, 78 (2003);  
E.V. Linder, *Astropart. Phys.* **29**, 336 (2008).
- [61] C. Blake, et al., *Mon. Not. Roy. Astron. Soc.* **415**, 2876 (2011).
- [62] R. Reyes, et al., *Nature* **464**, 256 (2010).
- [63] M. Tegmark, et al., *Phys. Rev. D* **74**, 123507 (2006).
- [64] N.P. Ross, et al., *Mon. Not. Roy. Astron. Soc.* **381**, 573 (2007).
- [65] L. Guzzo, et al., *Nature* **451**, 541 (2008).
- [66] J. da Angela, et al., *Mon. Not. Roy. Astron. Soc.* **383**, 565 (2008).
- [67] P. McDonald, et al., *Astrophys. J.* **635**, 761 (2005).

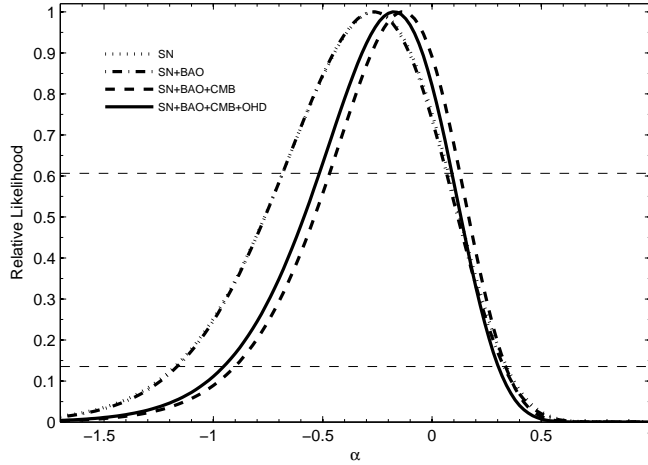


Figure 1: The 1D marginalized likelihood of  $\alpha$ . The horizontal dashed lines give the bounds with  $1\sigma$  and  $2\sigma$  CLs.

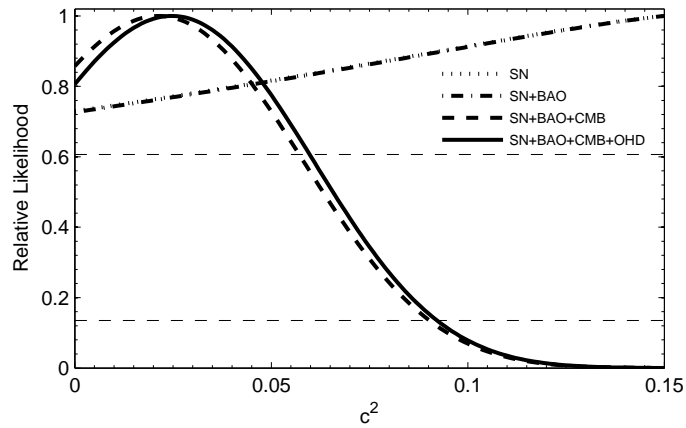


Figure 2: Same as Fig. 1 for the parameter  $c^2$ .

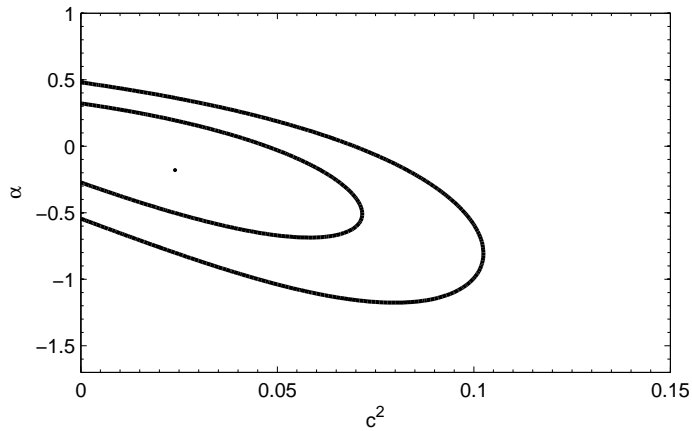


Figure 3: The 68.3% ( $1\sigma$ ) and 95.4% ( $2\sigma$ ) CL contours for  $\alpha$  versus  $c^2$  from the full data sets.

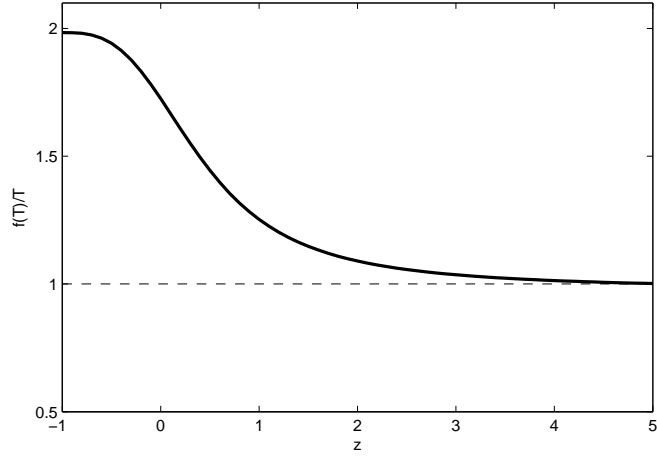


Figure 4: The evolution of PLECH  $f(T)$ -gravity model, Eq. (24), versus  $z$ . The dashed line denotes the model  $f(T) = T$  corresponding to the case of TG for comparison.

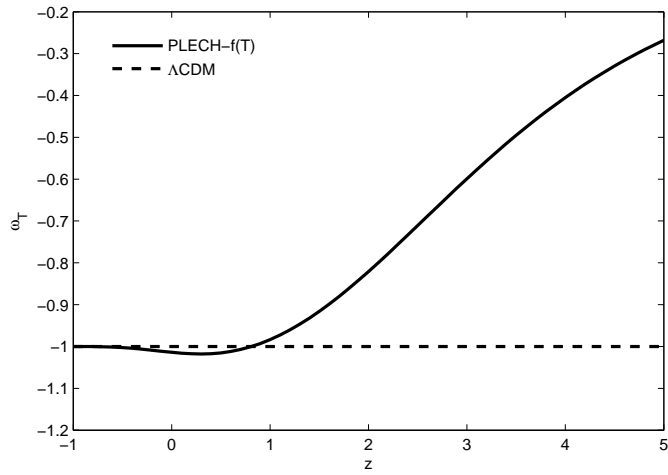


Figure 5: The effective torsion EoS parameter of the PLECH  $f(T)$ -gravity model, Eq. (30) and  $\Lambda$ CDM using the full data sets.

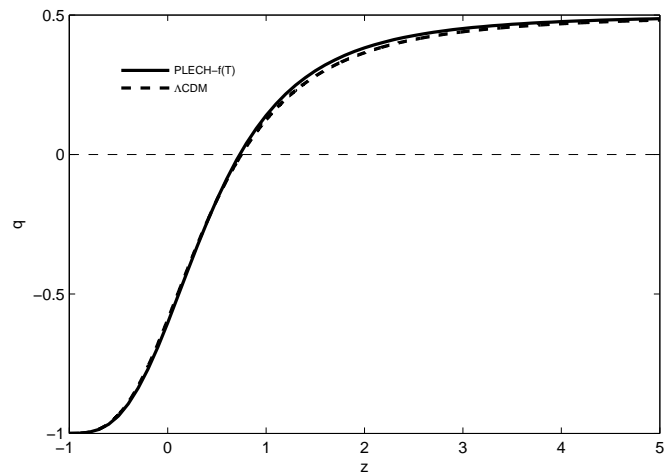


Figure 6: The best-fit of the deceleration parameter  $q(z)$  of the universe for the PLECH  $f(T)$ -gravity model, Eq. (31), and the  $\Lambda$ CDM model using the full data sets.

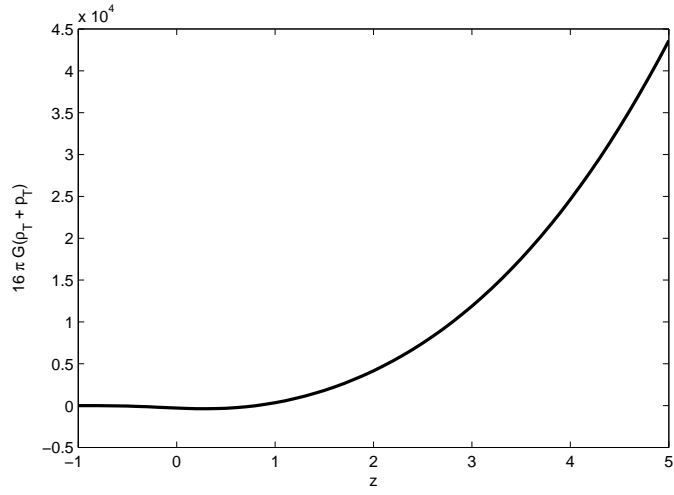


Figure 7: The evolution of  $\rho_T + p_T$  versus  $z$ .

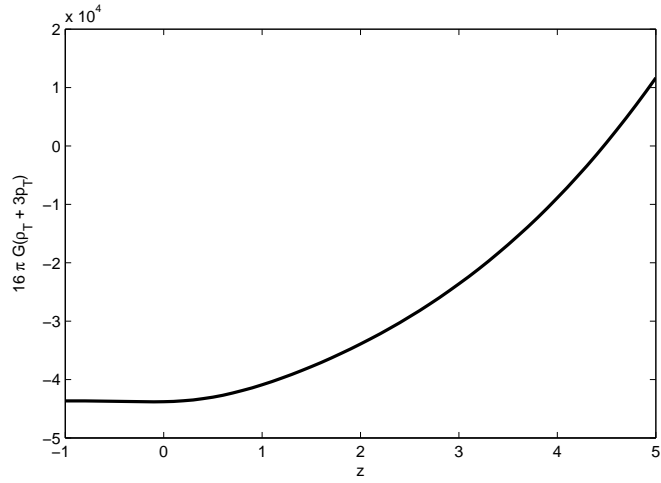


Figure 8: Same as Fig. 7 for  $\rho_T + 3p_T$ .

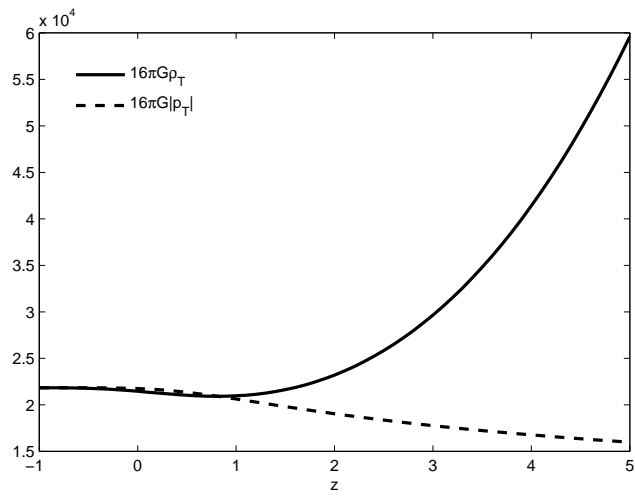


Figure 9: Same as Fig. 7 for  $\rho_T$  and  $|p_T|$ .

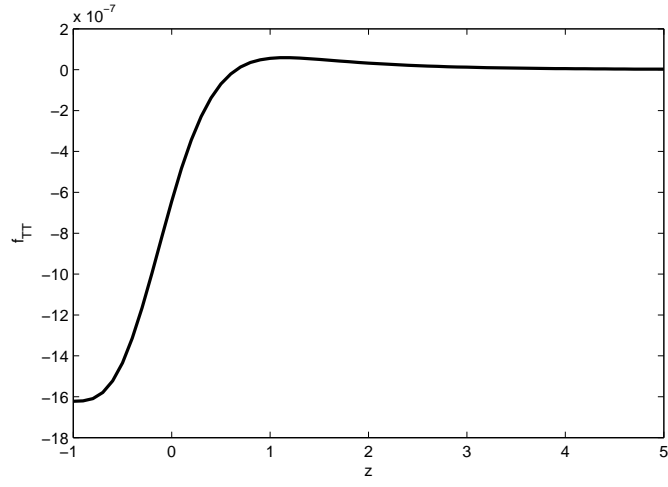


Figure 10:  $f_{TT}$  versus  $z$  for the PLECH  $f(T)$ -gravity model (24).

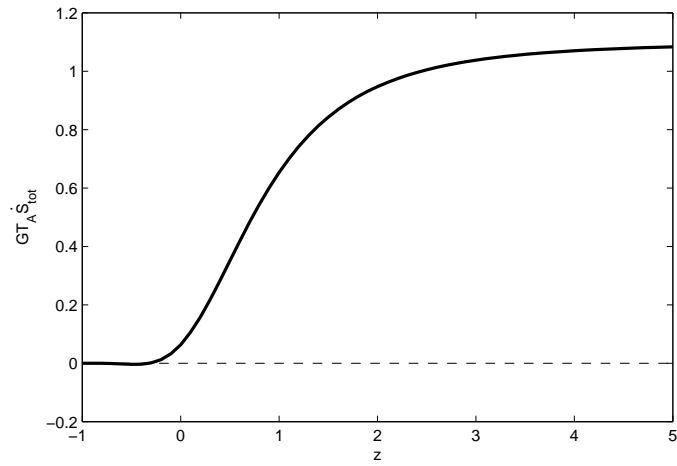


Figure 11: The variation of the GSL, Eq. (48), versus  $z$  for model (24).

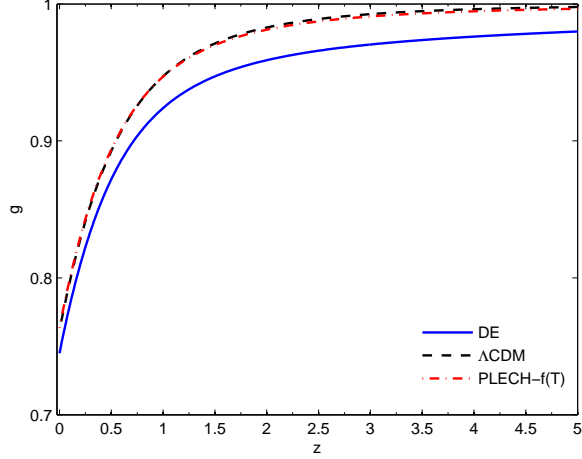


Figure 12: The variation of  $g(a) \equiv \delta_m/a$  versus  $z$  in the PLECH  $f(T)$ -gravity model,  $\Lambda$ CDM model, and DE model with the same EoS in GR.

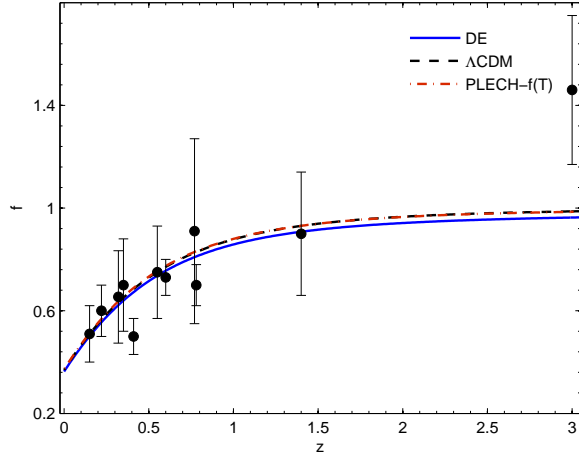


Figure 13: Evolution behaviors of the growth factor for the PLECH  $f(T)$ -gravity model,  $\Lambda$ CDM model, and DE model with the same EoS in GR.

Table 1: The observational  $H(z)$  data [51]-[53].

$z$	0	0.1	0.17	0.27	0.4	0.48	0.88	0.9	1.30	1.43	1.53	1.75
$H(z)$	74.2	69	83	77	95	97	90	117	168	177	140	202
$1\sigma$	$\pm 3.6$	$\pm 12$	$\pm 8$	$\pm 14$	$\pm 17$	$\pm 60$	$\pm 40$	$\pm 23$	$\pm 17$	$\pm 18$	$\pm 14$	$\pm 40$

Table 2: The best-fit values of the parameters  $\alpha$  and  $c^2$  within the 68.3% ( $1\sigma$ ) and 95.4% ( $2\sigma$ ) CLs for each observational data set for the PLECH  $f(T)$ -gravity model. Columns 5, 6, and 7 show the current effective torsion EoS parameter, the current deceleration parameter of the universe and the transition redshift, respectively. The last row shows the best-fit result of the  $\Lambda$ CDM model using the full data sets for comparison.

Data	$\alpha$	$c^2$	$\chi^2_{\min}$	$\omega_{T_0}$	$q_0$	$z_t$	$\chi^2/dof$
SN	$-0.26^{+0.34+0.60}_{-0.42-0.91}$	0.15	562.259	-0.97	-0.5	0.63	0.941
SN + BAO	$-0.26^{+0.33+0.59}_{-0.42-0.91}$	0.15	562.362	-0.97	-0.5	0.63	0.942
SN+BAO +CMB	$-0.14^{+0.27+0.48}_{-0.33-0.76}$	$0.021^{+0.036+0.069}$	562.381	-1.01	-0.6	0.74	0.942
SN+BAO+ CMB+OHD	$-0.18^{+0.27+0.48}_{-0.34-0.77}$	$0.025^{+0.035+0.067}_{-0.025-0.025}$	571.026	-1.01	-0.6	0.73	0.956
$\Lambda$ CDM	—	—	571.306	-1	-0.6	0.75	0.957

 Table 3: The observational data for the linear growth rate  $f_{\text{obs}}(z)$ .

$z$	0.15	0.22	0.32	0.35	0.41	0.55	0.60	0.77	0.78	1.4	3.0
$f_{\text{obs}}$	0.51	0.60	0.654	0.70	0.50	0.75	0.73	0.91	0.70	0.90	1.46
$1\sigma$	0.11	0.10	0.18	0.18	0.07	0.18	0.07	0.36	0.08	0.24	0.29
Ref.	[60]	[61]	[62]	[63]	[61]	[64]	[61]	[65]	[61]	[66]	[67]